



Observed spatiotemporal changes in air temperature, dew point temperature and relative humidity over Myanmar during 2001–2019

Zin Mie Mie Sein¹ · Irfan Ullah² · Vedaste Iyakaremye² · Kamran Azam³ · Xieyao Ma⁴ · Sidra Syed⁵ · Xiefei Zhi^{2,6}

Received: 27 March 2021 / Accepted: 23 September 2021 / Published online: 23 November 2021
© The Author(s), under exclusive licence to Springer-Verlag GmbH Austria, part of Springer Nature 2021

Abstract

Understanding the prevailing changes in temperature and relative humidity (RH) is of crucial importance for climate risk reduction and management. Despite their importance, trends and temperature variability associated with other climate variables over the Southeast Asian nation of Myanmar are not fully understood. This study investigates the annual and seasonal variations in air temperature and RH, as well as dew point temperature and their relationships, based on 47 meteorological stations located around Myanmar from 2001 to 2019. The results indicate that an increasing trend in air temperature was observed in the central, western, deltaic and southern regions of Myanmar. In contrast, air temperatures trended downward in the eastern (southern Shan state), northern (Hkakabo Razi Mountain) and western (Chin state) parts of the country. RH exhibited a significant increase in the northern region and a decrease in the central dry zone. A lower RH always accompanied high temperatures. Dew points increased in the deltaic and southern parts of Myanmar, as opposed to in the eastern (south Shan state) and western (Chin state) parts of the country. Moreover, in comparison to the daily RH variability, the observed daily temperature variability had a relatively stronger influence on Myanmar's climate, whereas dew points typically remained stationary for a day. The associated linkage between the RH and the dew point temperature was significantly linear, with a correlation coefficient (R^2) of 0.65. The annual (seasonal) correlation of air temperature and dew point was highly correlated in the winter, where R^2 was measured at 0.71 (0.75). During the rainy season, however, the annual (seasonal) R^2 was measured at only 0.30 (0.04). However, the air temperature and RH showed a weak positive correlation of 0.20 (0.26) in summer (winter) and a weak positive correlation in the rainy season (0.01). This study's findings are important for enhancing seasonal forecasts of extreme heat and can aid policy-makers in formulating better climate change adaptation plans.

Responsible Editor: Clemens Simmer.

✉ Irfan Ullah
irfan.marwat@nuist.edu.cn

✉ Xiefei Zhi
zhi@nuist.edu.cn

¹ College of International Students, Wuxi University, Wuxi 214105, Jiangsu Province, China

² School of Atmospheric Science, Nanjing University of Information Science and Technology, Nanjing 210044, China

³ Department of Management Sciences, University of Haripur, Khyber Pakhtunkhwa 22780, Pakistan

⁴ School of Hydrology and Water Resources, Nanjing University of Information Science and Technology, Nanjing 210044, China

⁵ Institute of Peace and Conflicts Studies, University of Peshawar, Peshawar 25000, Pakistan

⁶ Weather Online Institute of Meteorological Applications, Wuxi 214000, China

1 Introduction

Excluding the most widely cited variable of temperature, climate change can naturally also affect related variables such as relative humidity (RH) and wet-bulb, dry-bulb and dew point temperatures. These are affected by atmospheric sensible and latent heat and water vapour (Lawrence 2005; Ge et al. 2021). The surface air temperature and subsequent water vapours are essential components of climate change and the hydrological cycle. Temperature, RH, wind speed, precipitation and dew point temperature are identified as critical weather components in climate studies (Chawla et al. 2015; Akpan et al. 2016; Samarathna et al. 2017; Ukhurebor et al. 2017). Changes in one of these elements could also change others (Dailidé et al. 2019). For example, increasing global air temperature is likely to raise the concentration of water vapour as warmer air masses have a higher saturation vapour pressure (Iyakaremye et al. 2021a). Southeast Asia has recorded a mean surface temperature increase of between

0.14 and 0.20 °C per decade with increasing trends in the number of hot days and warmer nights, subsequently leading to an increase in the number of cold days and nights (Shi et al. 2021). Another weather parameter, water vapour, is one of the most important factors that influences the weather and climate due to its role as a greenhouse gas and the large amounts of energy involved as water changes between states (Schmidt et al. 2010; Seong et al. 2020). Water vapour plays an important role in hilly regions as opposed to flat regions through changes in precipitation, clouds (amount and height) and the amount of water from cloud droplet interception (Ge et al. 2021; Mie Sein et al. 2021b).

RH is a percentage that indicates how saturated the air is, whereas the dew point temperature is the temperature to which air must be cooled for condensation to occur (Huang et al. 2019). Humidity indicators such as RH and dew point temperature describe the moisture content of the atmosphere. Temperature, which is the thermal condition observed by a human, has been revealed to diverge according to the relative influence of humidity, wind and solar radiation (Lai et al. 2020; Jiang et al. 2020). RH and dew point temperature are broadly utilized indicators of water vapour in the air (Ali et al. 2018). The dew point is directly proportional to the water vapour quantity (Ukhurebor et al. 2017). If the dew point temperature is closer to the air temperature, then the air warms while the RH approaches 100% (Shrestha et al. 2019). Shrestha et al. (2019) reported that the dew point could be utilized to determine how much the temperature will drop during the night. As most water vapour in the atmosphere is limited near the surface (~2 km), the changes in near-surface RH are controlled to be relatively small, indicating that changes in precipitable water are dominated by changes in the near-surface saturation specific humidity. In addition, the dry-bulb temperature is the air temperature measured by a standard thermometer, and it reflects the cooling impact of dissipating water. RH directly affects atmospheric visibility and mainly influences the formation of clouds, fog and smog (Zheng et al. 2020). Moreover, RH is a function of the temperature and absolute water vapour concentration. Therefore, a change in RH could be described by a corresponding change in dew point temperature (T_{dew}). Recently, Mie Sein et al. (2021b) indicated that the RH exhibited a negative anomaly in the whole Southeast Asian region, while southern and eastern areas experienced a positive anomaly during the rainy season. Precipitable water changes occurred at approximately the rate detailed by the Clausius–Clapeyron relation, as seen in observed climate variations and simulated climate change scenarios (Gu et al. 2020). The Clausius–Clapeyron equation predicts an approximately 7% increase in the moisture holding capacity of the atmosphere per warming degree (Huo and Peltier 2020). Nasrollahi et al. (2018)

revealed that the annual RH has increased by 1.03 and 0.28 °C per decade in the northern and southern coastal regions of Iran, respectively, while the annual dew point temperature has increased by 0.29 and 0.15 °C per decade in the northern and southern coastal areas of Iran, respectively. Alamgir et al. (2020) studied the changes in annual and seasonal RH and dew point temperature at 15 stations across Bangladesh during 1961–2010. The results showed that significant negative trends in RH were apparent in the monsoon season. A 0.79 coefficient of determination between the RH and the dew point temperature was revealed in Benin City (Ukhurebor et al. 2017).

Generally, Myanmar has three seasons: a March–April summer, a May–October rainy season and a November–February winter season. The country is characterized by eight geographical regions: (1) Northern Hilly, (2) Central Dry, (3) Rakhine Coastal, (4) Western Hilly, (5) Eastern Hilly (Shan Plateau), (6) the Ayeyarwady Delta, (7) Yangon Deltaic and (8) Southern Coastal (Mie Sein et al. 2015). Myanmar experiences natural disasters almost every year due to high temperatures in the summer that can cause drought, heatwaves and water scarcity (Sein et al. 2021). Kreft et al. (2017) stated that Myanmar experienced maximum temperature records ranging between 40–45 °C and 37.465 °C in April–May 2010 and 2016, respectively. Sein and Zhi (2016) show that the country has experienced various climate hazards/extreme weather events, such as extreme temperatures, drought, heatwaves and floods, in recent decades. Drought is the most severe weather event in the country, followed by extreme temperatures (Sein et al. 2021). Myanmar frequently experienced heatwaves from 1951 to 2000, with the most severe occurring in 1998 (NECC and MECF 2012). Eckstein et al. (2019) showed that globally, Myanmar had the highest air temperature and was affected by peak weather events during 1999 and 2018. Recently, Mie Sein et al. (2021a) argued that air temperature variability over Myanmar is a very important weather element for detecting anthropogenic climate change. Thus, it is important to study the spatial and temporal variations in air temperature, RH, dew point, and dry-bulb and wet-bulb weather parameters and their relationship over the region. A plethora of studies have indicated that on average, the Earth's temperature is rising, with this rise projected to continue throughout the twenty-first century (Iyakaremye et al. 2021b, c). This warming is mostly attributed to anthropogenic activities (Iyakaremye et al. 2021b). Consequently, assessing current monthly, seasonal and annual air temperatures; RH; dew points; wet- and dry-bulb temperatures; and the relationship between them in Myanmar will provide crucial reference points for policy-makers in terms of developing climate change adaptation plans. The remainder of this paper is structured as follows: Sect. 2 describes the study area, materials and methods. Section 3 presents the main findings of this study.

2 Materials and methods

2.1 Study area and data

Myanmar is a tropical country located in Southeast Asia and is located between 9°32'N–28°31'N and 92°10'E–101°11'E. The region is situated between the Indian Ocean and the Bay of Bengal in the west and the Philippine Sea, the South China Sea and the Pacific Ocean in the east (Mie Sein et al. 2015, 2021a; Ge et al. 2021). The country experiences high spatial variability in temperature due to multifaceted and diverse topography. The central region experiences the highest annual average temperature ($> 38\text{ }^{\circ}\text{C}$), while the southern and western parts of the country experience the coldest annual temperature ($< 0\text{ }^{\circ}\text{C}$) (Suman and Maity 2020; Mie Sein et al. 2021a). The study area and observed meteorological stations used in this study are presented in Fig. 1 and Table 1. The present study used daily mean air temperature, daily mean RH and daily mean dry-bulb and wet-bulb temperature datasets derived from 47 stations around Myanmar. The data span from 2001 to 2019. The data were obtained from the Department of Meteorology and Hydrology (DMH), Myanmar. The data from the 47 stations were selected based on longer temporal coverage, data homogeneity and completeness of the data record. Recent studies have stated that the use of a ground-based gridded dataset is a good choice for a comprehensive study of distinct climatic

factors in the target region (Ullah et al. 2021a; Shahzaman et al. 2021a). The application of gridded datasets for similar purposes is subjected to validation to document their capabilities and uncertainties (Shahzaman et al. 2021b). Furthermore, temperature variability and its behaviour in intricate landscapes and high latitudes are more complex. Therefore, the applications of such gauge-based gridded datasets from similar studies may generate uncertainties in the results (Suman and Maity 2020; Mie Sein et al. 2021a). However, sometimes, gridded data tend to underestimate or overestimate climatic factors' intensity and frequency, which may eventually affect their long-term trend in a region with a diverse landscape (Ahmed et al. 2018; Shahzaman et al. 2021a). Based on the above facts, this study used long-term in situ observations with a high-density station network over diverse and high-elevation regions.

2.2 Methods

The use of geographic information system (GIS) is an important step in providing additional spatial analytical capabilities (Anselin et al. 1993). This method was used in this study to present the climatology of the spatial distribution for air temperature, RH, and dry-bulb and wet-bulb and dew point temperatures. The average dew point temperature was calculated based on the daily temperature and RH datasets. Correlation analysis reveals simple relationships between pairs of variables and was used in this study. The correlation coefficient

Fig. 1 Elevation map of the study area with meteorological stations

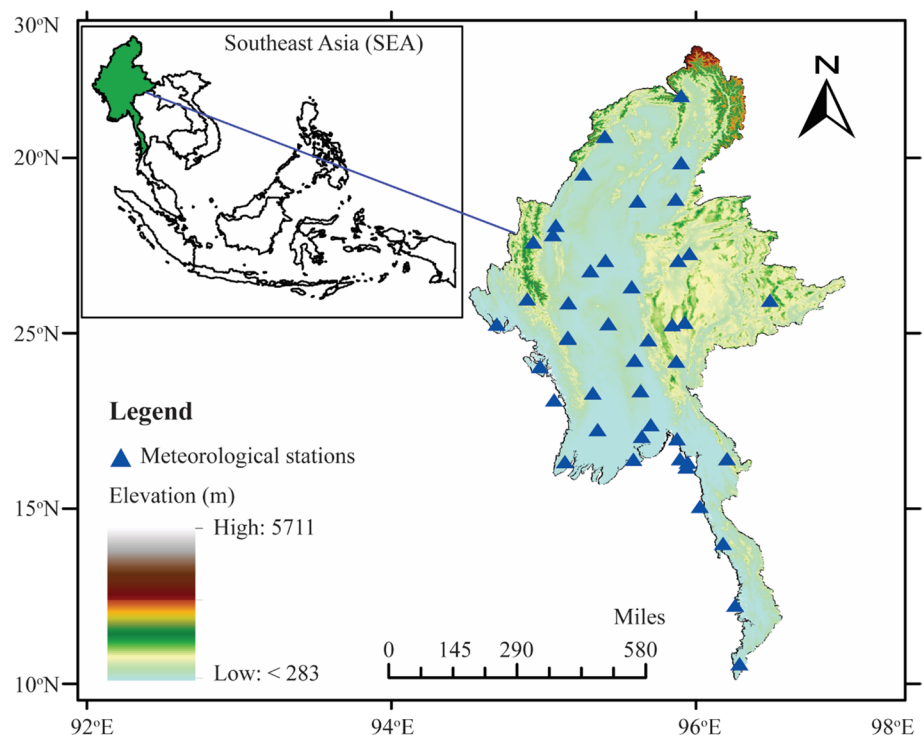


Table 1 Synoptic stations used in this study over Myanmar

| Number | Station name | Latitude (°N) | Longitude (°E) | Elevation (m) |
|--------|--------------|---------------|----------------|---------------|
| 1 | Monywa | 22.06 | 95.08 | 81 |
| 2 | Taunggyi | 20.47 | 97.03 | 1436 |
| 3 | Hmawbi | 17.02 | 92.00 | 5 |
| 4 | Putao | 27.20 | 97.25 | 409 |
| 5 | Myitkyina | 25.22 | 97.24 | 145 |
| 6 | Bago | 17.20 | 96.30 | 15 |
| 7 | Mandalay | 21.59 | 96.06 | 74 |
| 8 | Sittwe | 20.10 | 92.90 | 4 |
| 9 | Dawei | 14.08 | 98.20 | 16 |
| 10 | Patheingyi | 16.46 | 94.46 | 9 |
| 11 | Mingaladon | 16.54 | 96.11 | 28 |
| 12 | Mawlamyine | 16.30 | 97.37 | 21 |
| 13 | Bilin | 17.13 | 97.14 | 61 |
| 14 | Maungdaw | 20.82 | 92.37 | 6 |
| 15 | Magway | 20.07 | 94.53 | 52 |
| 16 | Hinthada | 17.40 | 95.25 | 13 |
| 17 | Tharrawaddy | 17.64 | 95.78 | 15 |
| 18 | Theinzayat | 17.51 | 96.88 | 11 |
| 19 | Monghsat | 20.52 | 99.25 | 580 |
| 20 | Loilem | 20.55 | 97.33 | 1355 |
| 21 | Loikaw | 19.41 | 97.13 | 895 |
| 22 | Homalin | 24.90 | 94.90 | 130 |
| 23 | Hkaha | 22.64 | 93.60 | 1866 |
| 24 | Kengtung | 21.18 | 99.37 | 827 |
| 25 | Lashio | 22.56 | 97.45 | 747 |
| 26 | Bhamo | 24.16 | 97.12 | 111 |
| 27 | Hsipaw | 22.36 | 97.18 | 436 |
| 28 | Falam | 22.91 | 93.67 | 1372 |
| 29 | Hkamti | 26.00 | 95.42 | 146 |
| 30 | Shwegyin | 17.93 | 96.88 | 12 |
| 31 | Hpa-an | 16.45 | 97.40 | 9 |
| 32 | Thaton | 16.55 | 97.22 | 17 |
| 33 | Taunggyi | 18.55 | 96.28 | 47 |
| 34 | Myeik | 12.43 | 98.60 | 36 |
| 35 | Kyaukpadaung | 19.40 | 93.60 | 5 |
| 36 | Thandwe | 18.50 | 94.30 | 9 |
| 37 | Pyaw | 18.48 | 95.13 | 58 |
| 38 | Kalaywa | 23.12 | 94.18 | 109 |
| 39 | Kalemyo | 23.19 | 94.02 | 152 |
| 40 | Myaukoo | 20.35 | 93.11 | 14 |
| 41 | Kabaaye | 16.54 | 96.10 | 20 |
| 42 | Yamethin | 20.43 | 96.10 | 199 |
| 43 | Naungoo | 21.12 | 94.55 | 312 |
| 44 | Myingyan | 21.47 | 95.39 | 60 |
| 45 | Yay | 15.20 | 97.90 | 3 |
| 46 | Minbu | 21.23 | 93.57 | 51 |
| 47 | Meiktila | 20.50 | 95.50 | 214 |

(r) ranges between -1 and 1 . When the value of r is $+1$ or -1 , it indicates a perfect positive or negative correlation between a given pairs of variables, respectively (Wilks 2007). The approximate wet-bulb temperature T_{WB} can be described by Eq. (1) (Sadeghi et al. 2013):

$$T_{WB} \cong \frac{-\varnothing + \sqrt{\varnothing^2 - 4\lambda\psi}}{2\lambda}, \quad (1)$$

where λ , \varnothing and ψ are empirical coefficients. As a tropical region, the T_{WB} is positive ($0^\circ \leq T_{WB} \leq 40^\circ\text{C}$), and these fixed conditions were $T_{WB} = 0$, $T_{WB} = \frac{T_a}{2}$ and $T_{WB} = T_a$. This is a logical choice because T_{WB} is always $\leq T_a$, whereas $T_a =$ dry-bulb temperature.

The relationships among the air temperature T_{DB} , wet-bulb temperature T_{WB} , relative humidity R_H (%) and dew point temperature T_{dew} can be expressed as follows:

$$\frac{R_H}{100} = \frac{e_s(T_{dew})}{e_s(T_{DB})} = \frac{e_s(T_{WB}) - \gamma P_a(T_{DB} - T_{WB})}{e_s(T_{DB})}, \quad (2)$$

where $e_s(T)$ denotes the saturation vapour pressure of water in air and is a function of temperature T ; γ is the psychrometric coefficient with an approximate value of $6.46 \times 10^{-4} \text{ }^\circ\text{C}^{-1}$ empirically with adequate ventilation (Simões-Moreira 1999); P_a is the atmospheric pressure (1013.25 hPa at sea level); R_H is the relative humidity; T_{dew} is the dew point temperature, T_{DB} is the air temperature, and T_{WB} is the wet-bulb temperature.

Water vapour dynamics are more important in warmer climates than in colder climates due to the atmospheric water vapour concentration normally increasing with surface temperature. This is a consequence of the rapid increase in the saturation vapour pressure with temperature. According to the Clausius–Clapeyron relation, a small change, dT , in temperature T leads to a fractional change in saturation vapour pressure, e^* as follows:

$$\frac{\delta e^*}{e^*} \approx \frac{L}{R_v T^2} \delta T, \quad (3)$$

where R_v is the gas constant of water vapour and L is the specific latent heat of vaporization. If one substitutes temperatures representative of near-surface air in the present climate, then the fractional increase in saturation vapour pressure with temperature is approximately 6–7% K^{-1} . That is, the saturation vapour pressure increases 6–7% if the temperature increases 1 K (Boer 1993; Held and Soden 2000; Wentz and Schabel 2000; Trenberth and Stepaniak 2003).

The mean dew point temperature is calculated as follows:

$$T_{\text{dew point}} = \frac{b \left(\left(\frac{aT}{b} + T \right) + \ln \text{RH} \right)}{a - \left(\left(\frac{aT}{b} + T \right) + \ln \text{RH} \right)}, \quad (4)$$

where $a = 17.27$, $b = 237.7$ and $\text{RH} = 0-1$.

Linear regression analysis is the most extensively used of all statistical techniques and is a statistical procedure for calculating the value of a dependent variable from an independent variable (Hope 2019; Omer et al. 2020; Hina et al. 2021; Ullah et al. 2021b). Linear regression analysis was used to investigate the association between RH and the dew point temperature over Myanmar in this study. Daily mean temperature, RH and the mean dew point temperature were examined by correlation analysis at annual and seasonal scales. The summer, rainy and winter seasons are defined as March–April (MA), May–October (MJJASO) and November–February (NDJF) (Nwe et al. 2020; Mie Sein et al. 2021b), respectively.

3 Results

3.1 Variation in dew point temperature, air temperature and relative humidity over Myanmar

The annual mean daily air temperature over Myanmar during 2001–2019 is shown in Fig. 2. Overall, the results indicated that the maximum and mean temperatures were high in the central, deltaic, southern and western coastal regions. However, observed relatively low temperatures can be seen in the eastern and western (Chin Hills) areas. Figure 2a reveals a maximum high temperature in the central dry zone (Mandalay, Magway and lower Sagaing regions), deltaic (Ayeyarwady, Yangon and Bago regions), western coastal (Rakhine state) and southern parts of Myanmar (Tanintharyi region and Mon and Kayin states). However, the maximum temperature was low in the high mountainous areas of eastern (Shan Plateau), western (Chin Hills) and northern (Hkakabo Razi Mountain) China. The highest maximum temperature observed in the central core region recorded at 32–34.5 °C, which covers the Mandalay, Magway, and lower Sagaing stations, while the lowest maximum temperature recorded in eastern, northern, and western areas covers the states of Shan, Kachin, and Chin stations at 22–24.5 °C, respectively. Myanmar experienced significantly high maximum temperatures over most regions, particularly in the central core region and coastal zone, such as the deltaic, southern and western coastal areas. However, hilly regions appeared to have low maximum air temperatures, which was consistent with landscape effects. Figure 2b shows the highest minimum temperature in the central dry zone (Mandalay region), western coast (Rakhine state), deltaic (Ayeyarwady

and Bago regions) and southern areas (Tanintharyi region and Mon and Kayin states) (20.7–23.4 °C), while the lowest minimum temperature was observed in the eastern (southern Shan state) and western areas (Chin state) (9.9–18.0 °C). The results showed significantly high minimum temperatures over the central dry zone, western coast, deltaic area and southern area. However, in comparison to the other areas, the central part of the region (i.e., Magway region) and Yangon deltaic area had lower minimum temperatures. These regions are closer to the Bay of Bengal (BOB) and the Andaman Sea, which can play an important role in water vapour transport. Moreover, hilly regions such as the Shan Plateau and Chin Hills were characterized by the lowest minimum air temperature due to the high latitudinal effect. The mean air temperature over Myanmar is high in the central dry zone, western coast, deltaic area and southern area (26.1–28.6 °C), while the lowest was observed in the eastern and western regions (16.4–21.2 °C) (Fig. 2c). The results show mixed behaviour based on high elevation and latitude, such as the hilly areas on the Shan Plateau. The Chin Hills had low air temperatures in low latitude areas, such as the central core region, and the coastal zone near the BOB Andaman Sea was characterized by the highest air temperature.

Figure 3 shows the spatial distribution of the mean dry-bulb, wet-bulb and dew point temperatures for 2001–2019. Overall, the results showed that dry-bulb, wet-bulb and dew point temperatures were high in the deltaic and southern areas. However, these temperatures decreased in the eastern (southern Shan state) and western areas (Chin state). The dry-bulb temperature was high in the central dry zone, western coast, deltaic area and southern area, while it was low in the western (Chin state) region. Figure 3a shows the mean dry-bulb temperature calculated in the morning at 9:30 am, which was high in the central dry zone (Mandalay, Magway and lower Sagaing), western region (Rakhine state), deltaic region (Ayeyarwady, Yangon and Bago) and southern region (Tanintharyi region and Mon and Kayin states). The highest temperatures of 26–28.6 °C were observed in the northern and southern regions of the country. The lowest temperatures of 15.7–18.3 °C occurred in the western part of the country. The mean wet-bulb temperature measured in the evening at 6:30 pm revealed that the temperature was high in the deltaic and southern regions and ranged from 24 to 26.7 °C, while low temperatures, ranging between 13.4° and 0.7 °C, were observed in the eastern (southern Shan state) and western (Chin state) regions, as shown in Fig. 3b.

Moreover, the mean dew point temperature was higher in the deltaic and southern regions, with records of 21.7–24.4 °C, while lower temperatures were observed in the eastern (south Shan state) and western (Chin state) regions at rates of 11.2–13.8 °C, (Fig. 3c). Thus, the country

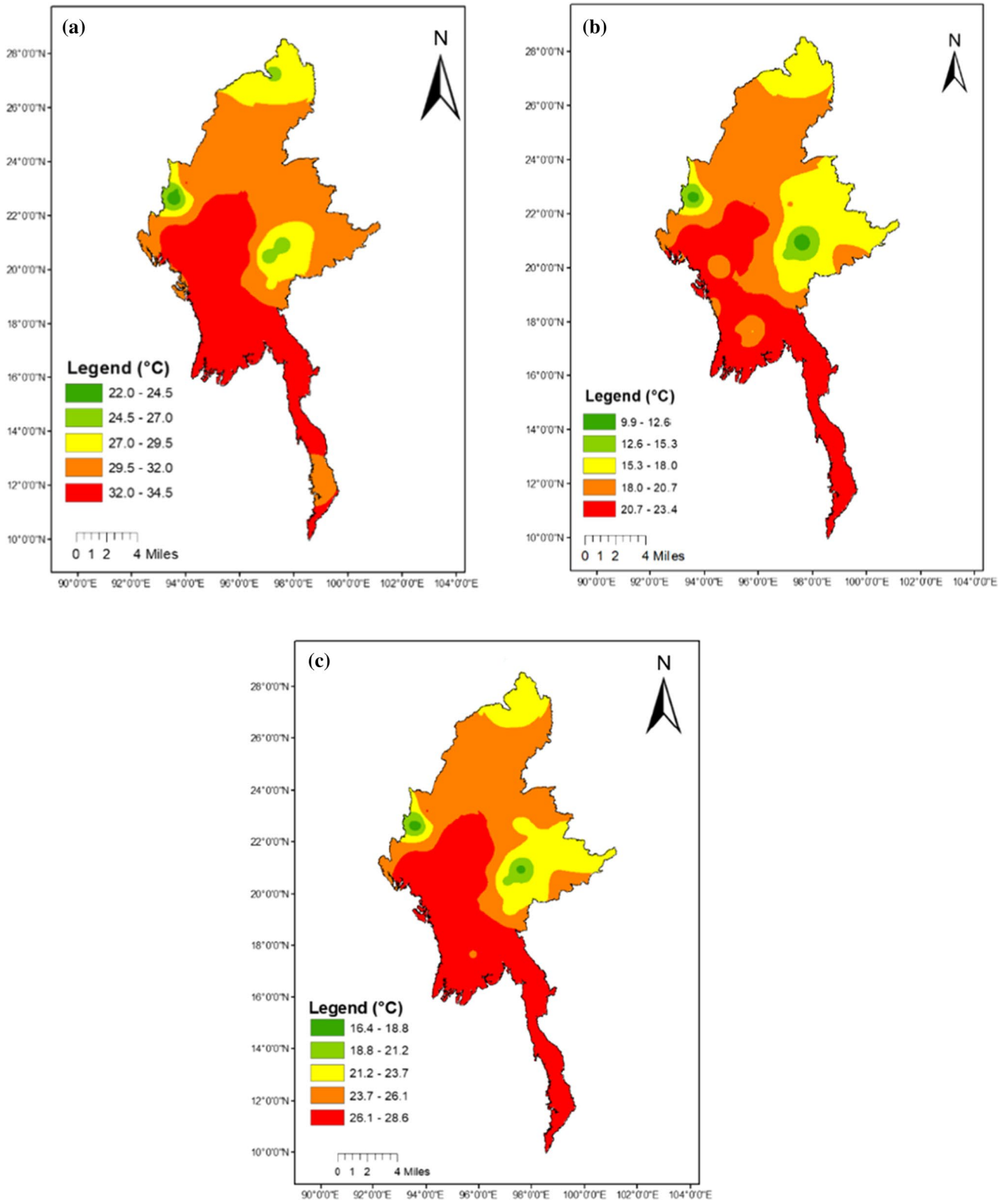


Fig. 2 Spatial distribution of annual mean daily air temperature over Myanmar (2001–2019) **a** maximum and **b** minimum temperatures and **c** mean temperature (°C)

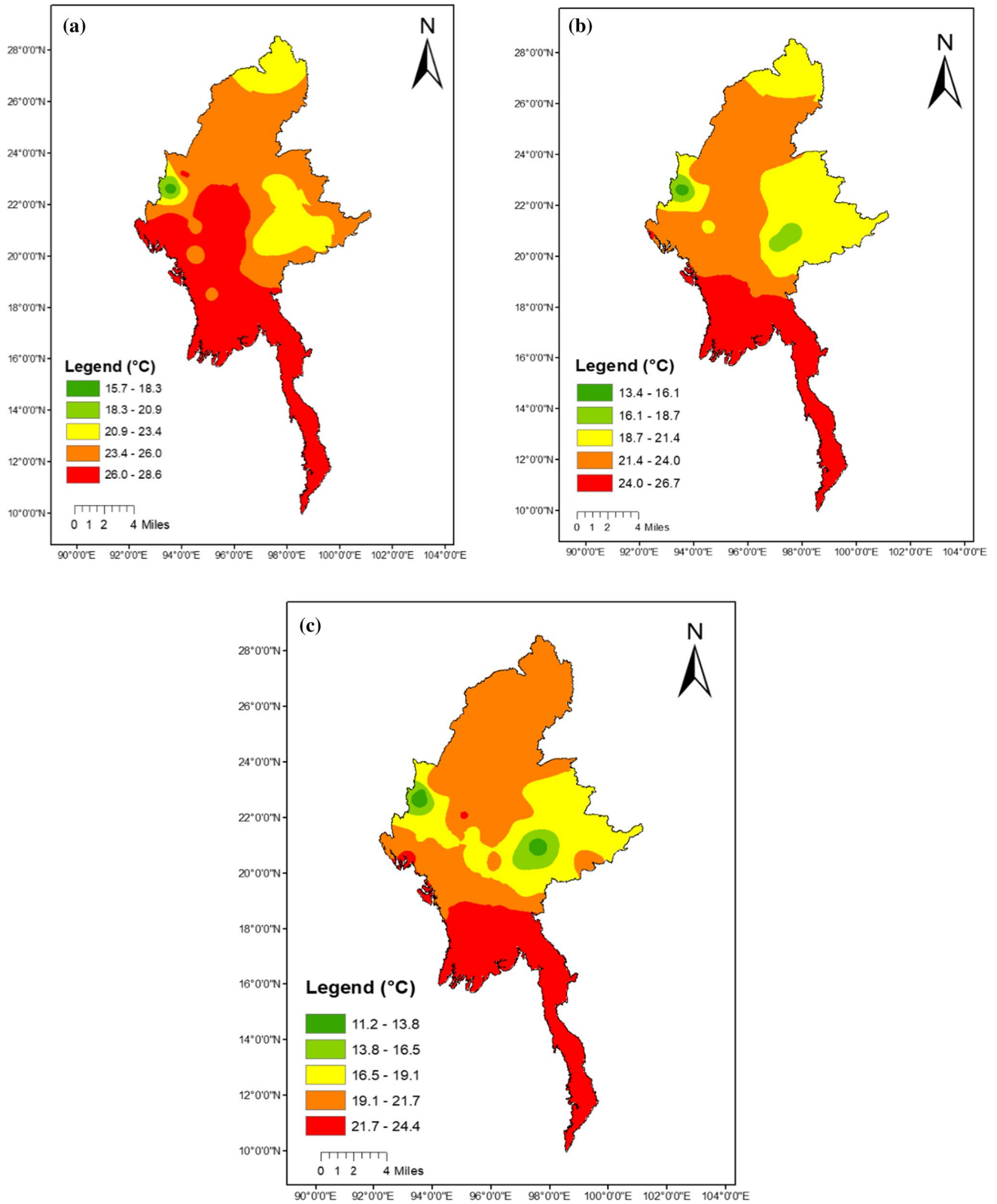


Fig. 3 Annual spatial distribution of temperature over Myanmar during 2001–2019: **a** mean dry-bulb temperature (°C), **b** mean wet-bulb temperature (°C) and **c** mean dew point temperature (°C)

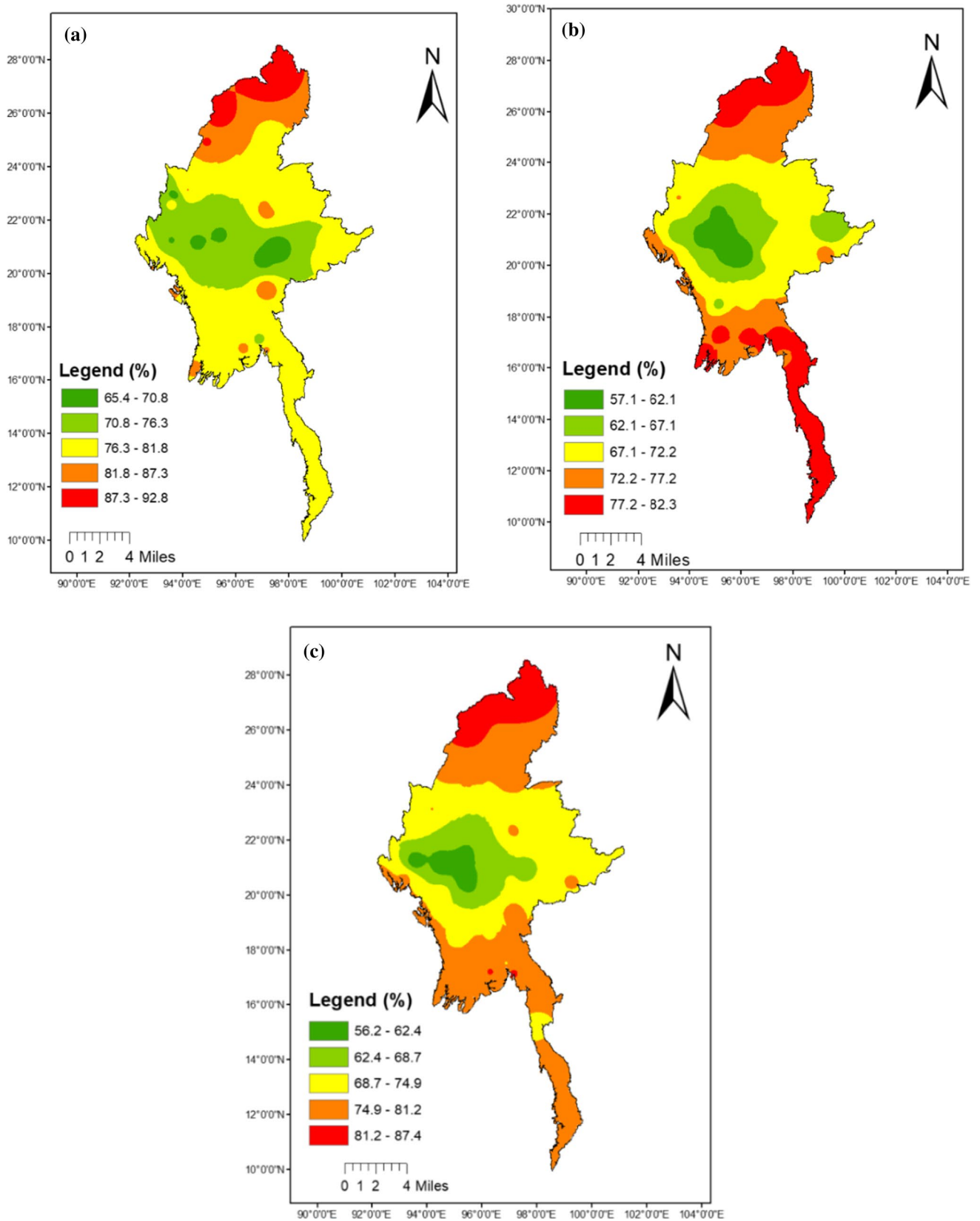


Fig. 4 Spatial distribution of RH (%) over Myanmar for 2001–2019 **a** RH at 9:30 am (%), **b** RH at 6:30 pm (%) and **c** mean relative humidity (%)

and its coastal areas influence the moisture transport or water vapour effect.

Figure 4 shows the observed mean RH at 9:30 am and 6:30 pm during 2001–2019. The results showed a significant decrease in the central dry zone and increases in the northern part of the target region. The RH in the morning at 9:30 am was high in northern Kachin state, ranging from 87.3% to 92.8%, while it was low in the central dry zone (Mandalay, Magway and lower Sagaing), eastern (Shan state) and western (Chin state) at 65.4%–76.3% (Fig. 4a). Additionally, the mean RH in the evening at 6:30 pm was high in the northern (Kachin state) and southern (Tanintharyi region and Mon and Kayin states) regions at 77.2%–82.3%, and relatively low RH of 57.1%–62.1% occurred in the central dry zone. The climatological mean RH was highest in northern Kachin (81.2%–87.4%) and lowest in the central dry zone

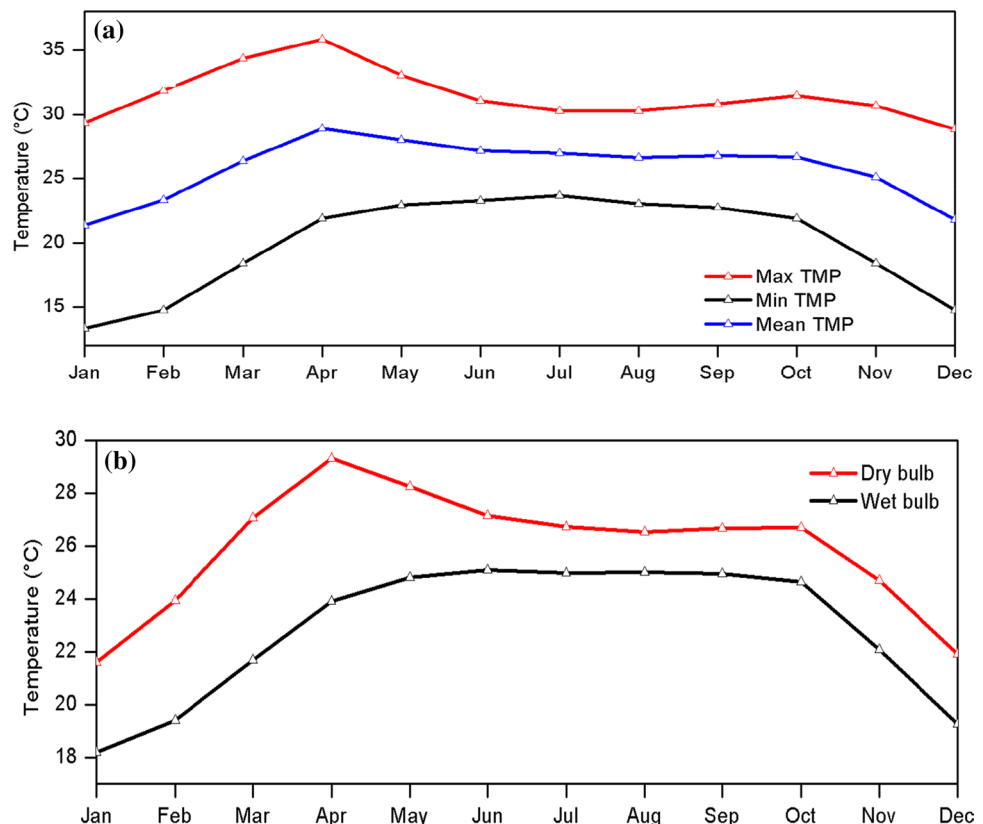
(56.2%–62.4%) (Fig. 4c). Therefore, it can be concluded that a low RH accompanied the warmest air temperature in areas such as the central dry zone. Table 2 provides the station results of the mean air temperature, dry-bulb and wet-bulb temperatures, dew point temperature and RH.

Figure 5 shows the annual cycle of daily mean air temperature (maximum, minimum and mean) and daily mean dry-bulb and wet-bulb temperatures over Myanmar during 2001–2019. Overall, the results indicated that the air temperature and dry-bulb temperature were highest in April and lowest in winter. However, minimum air temperature and wet-bulb temperature explained the hottest results in summer and the rainy season. Figure 5a reveals that the maximum air temperature increased in the summer (34–36 °C) but decreased in the winter at a rate of 29 °C. The minimum air temperature was high in both the summer and the rainy

Table 2 Annual mean air temperature (max, min and mean); dry-bulb, wet-bulb and dew point temperatures; and RH during 2001–2019

| Range | Air temperature (°C) | | | Dry bulb (°C) | Wet bulb (°C) | Dew point (°C) | Relative humidity (%) | | |
|---------|----------------------|---------------|--------------|---------------|---------------|----------------|-----------------------|------------|------------|
| | Max (6:30 am) | Min (3:30 pm) | Mean | 9:30 am | 6:30 pm | Mean | 9:30 am | 6:30 pm | Mean |
| Highest | 32–34.5 °C | 20.7–23.4 °C | 26.1–28.6 °C | 26–28.6 °C | 24–26.7 °C | 21.7–24.4 °C | 87.3–92.8% | 77.2–82.3% | 81.2–87.4% |
| Lowest | 22–0.5 °C | 9.9–18.0 °C | 16.4–21.2 °C | 15.7–20.9 °C | 13.4–18.7 °C | 11.2–13.8 °C | 65.4–76.3% | 57.1–67.1% | 56.2–68.7% |

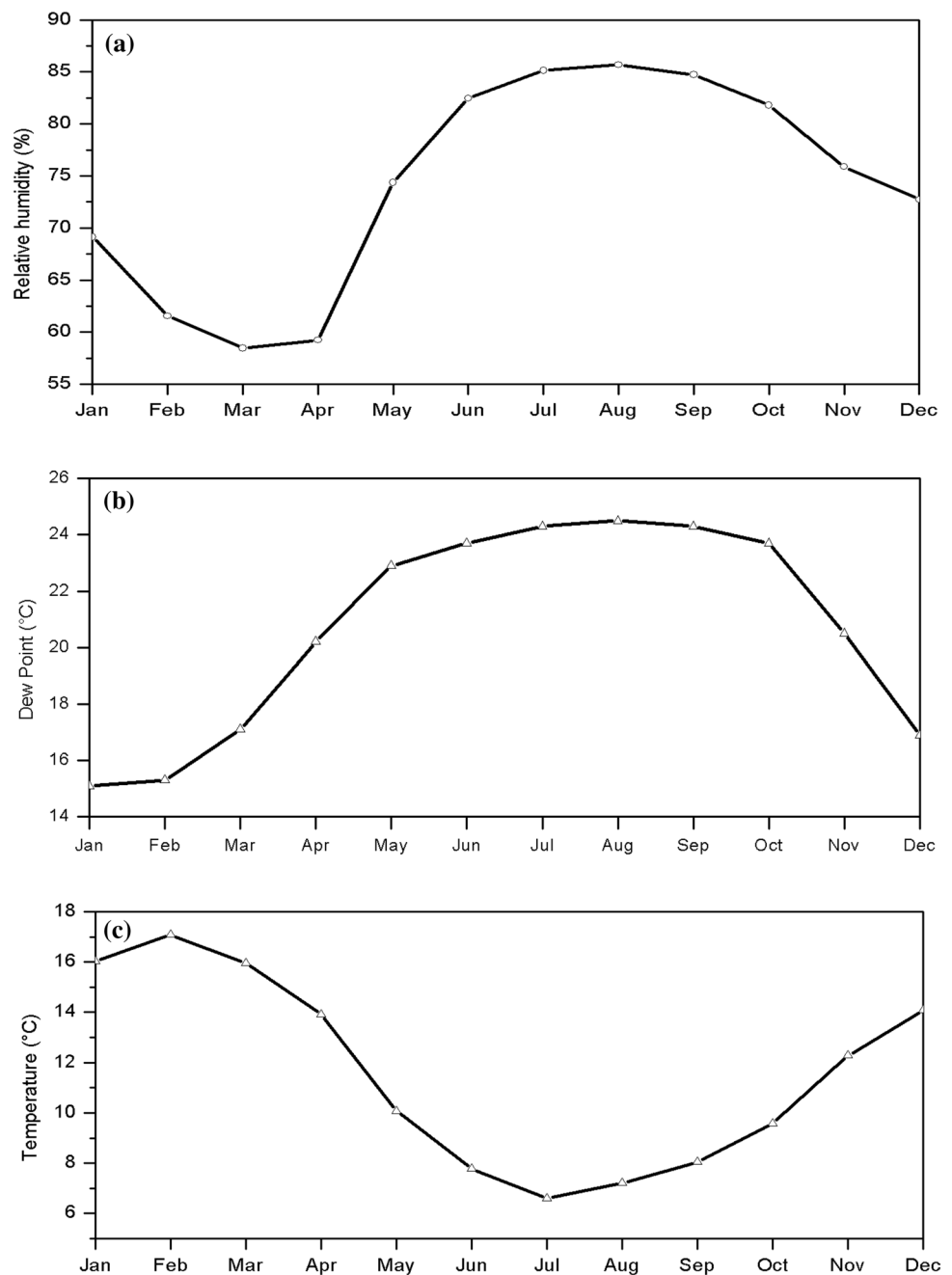
Fig. 5 Annual cycle **a** daily mean air temperature (maximum, minimum and mean) (°C) and **b** daily mean dry-bulb and wet-bulb temperatures (°C) (2001–2019)



season (22–24 °C) and decreased in the winter (13–15 °C) over the study region (Fig. 5a). The mean air temperature recorded generally increased in the summer (29 °C) and decreased in the winter (21–22 °C) (Fig. 5a). On average, the dry-bulb temperature results significantly increased in the summer season (April) (29 °C) and decreased in the winter season (22 °C) in the target region. The wet-bulb air temperature showed an increase in the summer and the rainy season (25 °C) and a decrease in the winter (18–19 °C) (Fig. 5b). Notably, the air temperature variation fluctuated from region to region during the different seasons.

Figure 6 shows the monthly variation in RH, dew point temperature and the difference in the maximum and minimum air temperatures during 2001–2019. Generally, RH and dew point temperature showed an increase in the rainy season spanning from June to October. However, RH decreased in the summer, and the dew point temperature decreased in the winter, as shown in Fig. 6a and b, respectively. In summary, daily temperature variability had a stronger influence on daily RH variability, as dew points typically remained fairly stationary for a day. The fluctuation in the temperature variance between the maximum and the minimum air temperature was significant (Fig. 6c). The difference between

Fig. 6 Monthly variation in the mean **a** RH, **b** dew point temperature (2001–2019), and **c** maximum and minimum air temperature difference during 2001–2019



daily maximum and minimum air temperatures gives the diurnal temperature range. During the rainy season, the air temperature is below 10 °C. This season is particularly characterized by a reasonable climatic situation according to rainfall and cloud formation in the rainy season. The summer and winter temperature differences were higher than 10 °C. The lowest temperature difference was observed in July (6.6 °C). Furthermore, the highest temperature difference occurred in February (17 °C), which was due to the lowest night-time temperature. This month was characterized by the extreme climatic situation that occurred in the region. Instabilities in the increase/decrease in RH and dew point temperature may be associated with the increasing (decreasing) trends in temperature, which may then affect the occurrence of extreme temperatures. The increase in the frequency and magnitude of extremely high temperatures, in addition to the decrease in the occurrence of low temperatures, may occur globally, which results in an increase in the length, frequency and intensity of warm periods or heat waves across the land (Wang et al. 2009; Grimaldi et al. 2018). Strong winds can transport water vapour from the ocean to nearby coastal areas, which can affect regional temperatures and ultimately affect cooling trends, and vice versa (IPCC 2014; Asmat and Athar 2017).

The seasonal mean air temperature (°C), dew point temperature (°C), and RH (%) for the summer, rainy season and winter season are shown in Fig. 7. The results provide the mean air temperature, which was the highest in the summer and rainy seasons (28–29 °C), while the dew point temperature was the highest in the rainy season (23–25 °C) (see Fig. 7). However, the air temperature (dew point temperature) was the lowest in the winter at approximately 21–22 °C (15–17 °C). Moreover, the RH was highest in the rainy season (82.4%) and lowest in summer (58.9%, Fig. 7). Therefore, the results indicated that the hottest temperatures will always have a lower RH simply because more water vapour is exponentially needed to achieve saturation (Kreft et al. 2017; Nwe et al. 2020; Ullah et al. 2021b). Table 3 further provides the specific values of seasonal air temperature

(maximum, minimum and mean); dry-bulb, wet-bulb, and dew point temperatures; and RH.

3.2 Relationship among mean air temperature, dew point temperature and relative humidity

The result of the trend and the relationship between RH (%) and dew point temperature (°C) (2001–2019) over Myanmar is shown in Fig. 8. The trend in RH and the dew point temperature against months are shown in Fig. 8a. Furthermore, the analysis of the association between RH (%) and dew point temperature (°C) is represented by a scatter plot in Fig. 8b. The association between the RH and the dew point temperature was linear with a significant coefficient of determination (R^2) of approximately 0.65, which supports the findings of previous work reported by (Ukhurebor et al. 2017; Mie Sein et al. 2021a, b). The result indicates that in comparison to other factors, daily temperature variability appeared to have stronger control on daily RH, as dew points will typically remain stationary for a day.

The annual mean air temperature, RH and dew point over Myanmar during 2001–2019 are shown in Table 4. The mean air temperature over Myanmar was the warmest in 2005 and 2010 (25.9 °C), while the coldest air temperature occurred in 2008 (25.3 °C) (see Table 4). Moreover, the average RH was highest in 2008 (76.3%) and lowest in 2004 (73.5%), while the average dew point temperature was highest in 2009 and 2010 (21.4 °C) and lowest in 2007 (20.3 °C). Table 5 presents the seasonal mean air temperature, dew point temperature and RH during 2001–2019 over the study area. Overall, the results showed that the mean air temperature was highest in the summer (27.6 °C) and lowest in the winter (22.8 °C) (see Table 3). The mean dew point temperature was the highest in the rainy season (23.7 °C) and the lowest in the winter (17.0 °C). The mean RH was highest in the rainy season (82.4%) and lowest in summer (58.9%). Moreover, the correlation (annual and seasonal) analysis between daily mean temperature and RH and dew point temperature is presented in Table 6. The correlation of the annual mean

Fig. 7 Seasonal mean summer (MA), rainy (MJJASO) and winter (NDJF) air temperature (°C), dew point (°C) and RH (%) over Myanmar

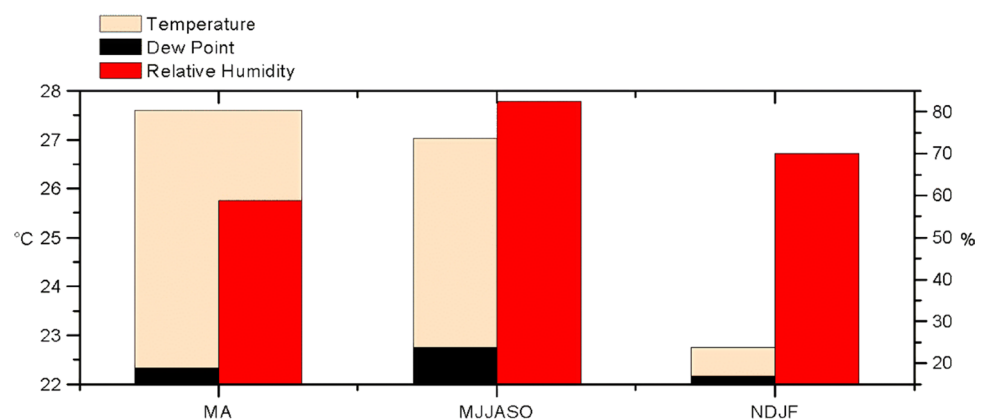


Table 3 Seasonal air temperature (max, min and mean); dry-bulb, wet-bulb, dew point temperatures; and RH from 2001–2019

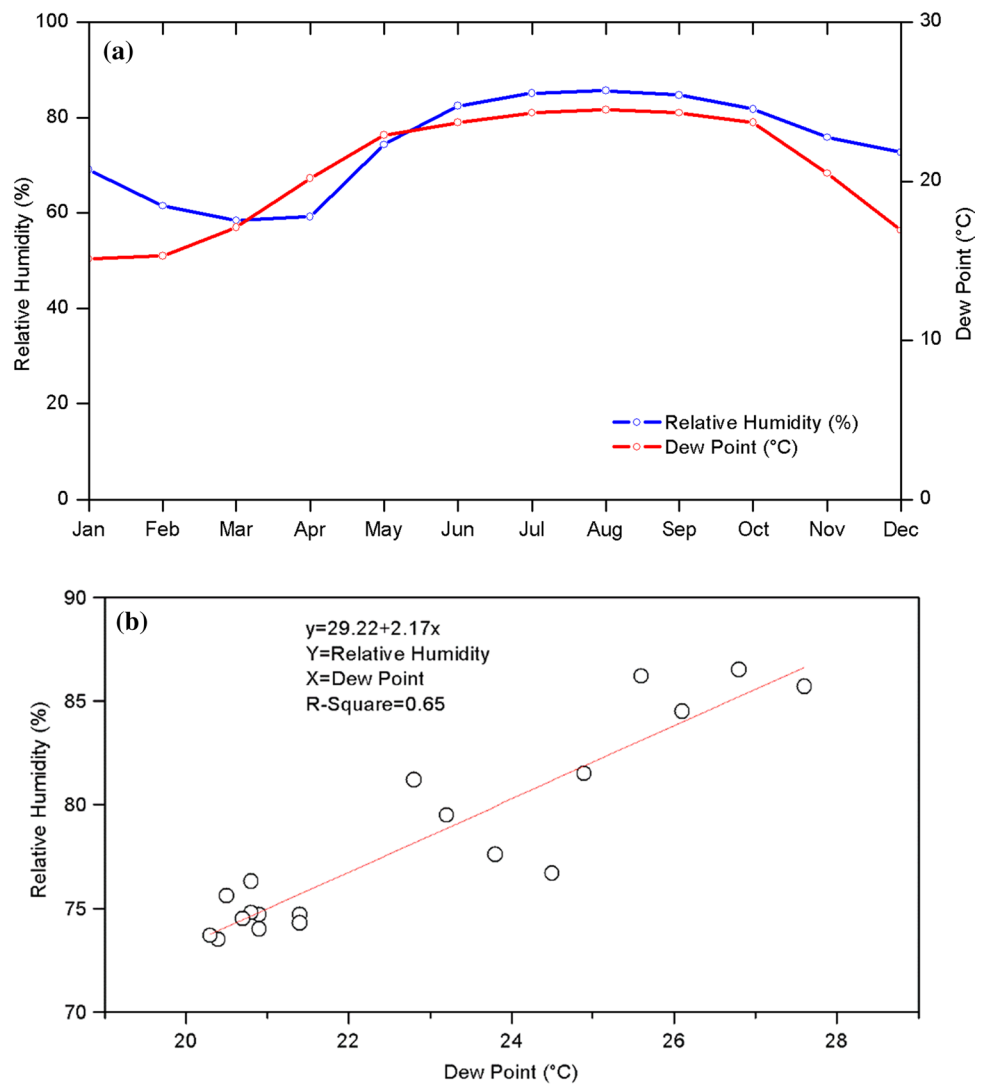
| Range | Air temperature (°C) | | | Dry bulb (°C) | | | Wet bulb (°C) | | | Dew point (°C) | | | Relative humidity (%) | | |
|---------|----------------------|----------|----------|---------------|--------|-------|---------------|----------|--------|----------------|--------|--------|-----------------------|------|--|
| | Season | Max | Min | Mean | Season | Mean | Season | Mean | Season | Mean | Season | Mean | Season | Mean | |
| Highest | Summer-rainy | 34–36 °C | 22–24 °C | 28–29 °C | Summer | 29 °C | Summer-rainy | 25 °C | Rainy | 23 °C–25 °C | Rainy | 82–86% | Rainy | | |
| Lowest | Winter | 29 °C | 13–15 °C | 21–22 °C | Winter | 22 °C | Winter | 18–19 °C | Winter | 15 °C–17 °C | Summer | 58–59% | Summer | | |

air temperature and dew point temperature showed a high positive correlation, with a correlation coefficient of 0.71. In contrast, the mean air temperature and RH showed a weak negative correlation, with a correlation coefficient of 0.30. Moreover, the seasonal correlation between daily mean air temperature and dew point temperature exhibited the highest positive correlation in winter (November–February), with a correlation of 0.75, while the lowest correlation in the rainy (May–October) season was ~ 0.04 . The correlation of seasonal daily air temperature and RH showed a weak positive correlation in summer (winter) at 0.20 (0.26), and a very weak positive correlation occurred in the rainy season (0.01) (see Table 6).

4 Discussion

The present study examined air temperature variability, dry-bulb and wet-bulb temperature, RH, dew point temperature and their relationship based on gauge-based gridded synoptic observed (47) station data during 2001–2019. The climate variables used in this study were analysed using Pearson correlation, linear regression and scatter plots and displayed using GIS. The results indicated that generally, the air temperatures were higher in the central dry zone, western coast, deltaic, and southern regions, whereas relatively low temperatures appeared in the eastern, northern and western parts of the country, such as in high mountainous regions of Hkakabo Razi Mountain, on Shan Plateau and in Chin Hills. The results indicate that the topography of the study domain mainly influenced the air temperature variations. The increase/decrease in air temperature in these regions and overall variability agree with the findings of other regional studies (Horton et al. 2017; Zheng et al. 2017; Suman and Maity 2020). The temperature difference between the daily maximum and minimum temperatures is defined with respect to the diurnal temperature range. During the rainy season, the air temperature was below 10 °C. This season was particularly characterized by a reasonable climatic situation according to rainfall and cloud formation in the rainy season. Differences between the summer and winter temperatures were 10 °C. The lowest temperature difference was observed in July (6.6 °C) over the target region. Similar results in regions near Nepal indicated differences between maximum and minimum temperatures below 10 °C. The lowest temperature difference was observed in July (5.97 °C) (Horton et al. 2017; Shrestha et al. 2019; Suman and Maity 2020). The highest temperature difference occurred in February (17 °C), indicating an extremely low night temperature (minimum) in the region. Moreover, the seasonal air temperature and dew point increased in the summer and rainy seasons and decreased in the winter. Thus, the summer in this tropical country occurs in the area of

Fig. 8 **a** Trend graph for RH (%) and dew point temperature (°C) and **b** the relationship between RH (%) and dew point temperature (°C) over Myanmar (2001–2019)



Myanmar that is in the Tropic of Cancer (the northernmost latitude where the sun can be straight overhead), and the rainy season occurs in areas where the intertropical convergence zone (ITCZ) exists. Recently, Nwe et al. (2020) described that most climatic zones show abrupt changes in air temperature over high-elevation regions where projected changes are observed with new bioclimatic conditions under a changing climate. They also noted that Myanmar needs proper protection of these areas; however, some influential factors, such as political interference and socioeconomic problems, make this protection difficult.

Moreover, RH is highest during the rainy season (May–October) of ~82.4% and is lowest in the summer season (March–April), at ~58.9% over the region. The results indicated high moisture transport from the BOB during the southwestern monsoon season. In this context, the region receives high moisture transport during the southwestern monsoon season, which further supports the findings of previous work conducted in the region (Sein and Zhi 2016;

Sein et al. 2021; Mie Sein et al. 2021a; Liu et al. 2021). Therefore, water vapour plays an important role in the climate variability in any part of the region. The association between the RH and the dew point temperature was linear, with a significant coefficient of determination (R^2) 0.65. The results further indicated that an increase or decrease in the RH would also convey an increase or decrease in the dew point and vice versa. Consequently, daily temperature variability will be a stronger control on daily RH variability, as dew points will typically remain stationary for a day. The correlation of the annual mean air temperature and dew point temperature showed a significantly high positive correlation, with a correlation coefficient of 0.71 over the target region. In contrast, the mean air temperature and RH showed a weak negative correlation, with a correlation coefficient of 0.30. Moreover, the seasonal correlation between daily mean air temperature and dew point temperature exhibited the highest positive correlation in the winter (0.75), while the lowest correlation appeared in the rainy season (approximately

Table 4 Annual mean air temperature (TMP), relative humidity (RH) and dew point (DP) (2001–2019)

| Year | TMP (°C) | RH (%) | DP (°C) |
|------|----------|--------|---------|
| 2001 | 25.7 | 74.7 | 20.9 |
| 2002 | 25.6 | 74.8 | 20.8 |
| 2003 | 25.6 | 74.5 | 20.7 |
| 2004 | 25.5 | 73.5 | 20.4 |
| 2005 | 25.9 | 74.0 | 20.9 |
| 2006 | 25.6 | 75.6 | 20.5 |
| 2007 | 25.4 | 73.7 | 20.3 |
| 2008 | 25.3 | 76.3 | 20.8 |
| 2009 | 25.8 | 74.7 | 21.4 |
| 2010 | 25.9 | 74.3 | 21.4 |
| 2011 | 24.6 | 79.5 | 23.2 |
| 2012 | 26.5 | 81.2 | 22.8 |
| 2013 | 27.3 | 86.2 | 25.6 |
| 2014 | 28.1 | 76.7 | 24.5 |
| 2015 | 26.7 | 84.5 | 26.1 |
| 2016 | 25.6 | 77.6 | 23.8 |
| 2017 | 27.6 | 81.5 | 24.9 |
| 2018 | 29.5 | 86.5 | 26.8 |
| 2019 | 29.8 | 85.7 | 27.6 |

Table 5 Seasonal mean air temperature (TMP), dew point temperature (DP) and relative humidity (RH), where values with bold indicate significance

| Seasons | TMP (°C) | DP (°C) | RH (%) |
|---------|-------------|-------------|-------------|
| MA | 27.6 | 18.9 | 58.9 |
| MJJASO | 27.0 | 23.7 | 82.4 |
| NDJF | 22.8 | 17.0 | 69.9 |

Table 6 Annual and seasonal correlations between mean temperature, relative humidity and dew point temperature

| Variables | Annual | Summer (MA) | Rainy (MJJASO) | Winter (NDJF) |
|--|--------|-------------|----------------|---------------|
| Mean air temperature vs. relative humidity | 0.30 | 0.20 | 0.01 | 0.26 |
| Mean air temperature vs. dew point temperature | 0.71 | 0.47 | 0.04 | 0.75 |

0.04). On the other hand, seasonal daily air temperature and RH had a relatively weak positive correlation of approximately 0.20 (0.26) in the summer (winter). A very weak positive correlation can be seen for the rainy season at 0.01. A similar result was shown in a previous study over China. Huang et al. (2019) and Zhang et al. (2019) reported that the

RH was weakly correlated with daily mean temperature at the interannual timescale in four seasons. An assessment at a seasonal scale could enhance the understanding of climate extremes such as floods and droughts (Hina et al. 2021; Liu et al. 2021). Moreover, such an assessment can also help increase economic growth, agricultural production, ecology and water resource management and preserve natural habitat in the target region. The role of climate extremes over East Asia and the surrounding areas discussed in (Ge et al. 2019, 2021; Zhu et al. 2019, 2020; Shim et al. 2021) provides an outlook into future climates. For example, (Ge et al. 2021) found projected changes in precipitation extremes likely linked to warmer futures over Southeast Asia (SEA). Earlier results by (Ge et al. 2019) found a high sensitivity of precipitation to be caused by a projected increase of 0.5 °C in global warming levels (GWL) from 1.5 to 2 °C. A similar study by (Shim et al. 2021) found that changes in extreme precipitation associated with a warming climate are becoming more intense and frequent in southern China based on CMIP6 scenarios. This is not surprising, as (Shim et al. 2021), using multi-RCM, observed that extreme precipitation is projected to follow enhanced moisture availability with warming. Moreover, (Zhu et al. 2020) presented temperature indices that increase significantly over SEA and occur at more pronounced magnitudes at a 2 °C GWL based on the ensemble of CORDEX simulations.

Our research provided annual (seasonal) variations in air temperature, RH, dew point temperature and their relationship in Myanmar that local governments can use to implement climate change policy and disaster risk management in the region.

The study does not contradict the potential impact of different climate variables but rather postulates that these controls need to be reviewed in terms of their clear links with summer monsoon variability over Myanmar and the region. Another reason to review these controls is that station data quality is recorded for synoptic-scale use, and climatological processes usually occur on a longer time scale. Thus, it may lack such large-scale variability. These are some points that need to be thoroughly investigated in future studies, including the frequency and intensity of extreme temperature events and their role as drivers of regional temperature variability.

5 Conclusions

This study explores the spatiotemporal variability in air temperature, dry-bulb and wet-bulb temperatures, dew point temperature and RH and their relationships during 2001–2019 over Myanmar. Using statistical analysis, the study found variations in different climatic variables at annual and seasonal scales. Air temperature was observed

to undergo a significant increase in the central dry zone, western coast, deltaic area and southern area of the region. Minor decreases were observed over mountainous regions such as the eastern, northern and western regions. The RH spatial variation indicated a substantial decrease in the hottest region and increases in RH in the cold region, especially in the northern part of the study area. Moreover, the RH increased in the rainy season and decreased in the summer. The dew point increased in the deltaic and southern areas, and a reduction occurred in the eastern and western areas. The relationship between the RH and the dew point temperature was found to be linear. The correlation of the annual mean air temperature and dew point temperature had a high positive association, with a correlation coefficient of 0.71.

In contrast, the mean air temperature and RH showed a relatively weak negative correlation of 0.30. Moreover, the seasonal correlation between daily mean air temperature and dew point temperature had the highest positive correlation of approximately 0.75 in the winter, while the lowest correlation of ~ 0.04 occurred in the rainy season. The correlation of seasonal daily air temperature and RH had a weak positive correlation in summer (winter) seasons at 0.20 (0.26) and a very weak positive correlation in the rainy season at 0.01. Even though the station data are subjected to deviation and uncertainties, the current study has reported diverse variabilities in the temperature and RH. Thus, an in-depth study is recommended to model the atmospheric mechanisms responsible for such high fluctuations in temperature over Myanmar.

Acknowledgements The National Natural Science Foundation of China with Grant No: 41877158 financially supported this work. The National (Key) Basic R&D Program of China with Grant No: 2012CB955204 also supports this study. Furthermore, this research was encouraged by the College of International Students, Wuxi University, Wuxi, Jiangsu Province, China. Special appreciation goes to the Department of Meteorology and Hydrology, Myanmar, for the provision of the datasets used in the study. We also thank the four anonymous reviewers for their constructive and thoughtful suggestions and comments.

Data availability The datasets generated during and/or analyzed during the current study are available from the corresponding author on reasonable request.

References

- Ahmed K, Shahid S, Nawaz N (2018) Impacts of climate variability and change on seasonal drought characteristics of Pakistan. *Atmos Res* 214:364–374. <https://doi.org/10.1016/j.atmosres.2018.08.020>
- Akpan V, Osakwe R, Ekong SA (2016) A hypothetical database-driven web-based meteorological weather station with dynamic datalogger system
- Alamgir M, Khan N, Shahid S et al (2020) Evaluating severity–area–frequency (SAF) of seasonal droughts in Bangladesh under climate change scenarios. *Stoch Environ Res Risk Assess* 34:447–464. <https://doi.org/10.1007/s00477-020-01768-2>
- Ali H, Fowler HJ, Mishra V (2018) Global observational evidence of strong linkage between dew point temperature and precipitation extremes. *Geophys Res Lett* 45:12320–12330. <https://doi.org/10.1029/2018GL080557>
- Anselin L, Dodson RF, Hudak S (1993) Linking GIS and spatial data analysis in practice. *Geogr Syst* 1:3–23
- Asmat U, Athar H (2017) Run-based multi-model interannual variability assessment of precipitation and temperature over Pakistan using two IPCC AR4-based AOGCMs. *Theor Appl Climatol* 127:1–16. <https://doi.org/10.1007/s00704-015-1616-6>
- Boer GJ (1993) Climate change and the regulation of the surface moisture and energy budgets. *Clim Dyn*. <https://doi.org/10.1007/BF00198617>
- Chawla A, Bangera T, Kolwalkar C, Bhat M (2015) Bluetooth based weather station. *Int J Eng Trends Technol* 28(2):98–101. <https://doi.org/10.14445/22315381/ijett-v28p219>
- Dailidė R, Povilanskas R, Pérez JAM, Simanavičiūtė G (2019) A new approach to local climate identification in the Baltic sea's coastal area. *Baltica*. <https://doi.org/10.5200/baltica.2019.2.8>
- Eckstein D, Hutfils M-L, Wings M (2019) The global climate risk index 2019: who suffers most from extreme weather events? Weather-related Loss Events in 2017 and 1998 to 2017
- Ge F, Zhu S, Peng T et al (2019) Risks of precipitation extremes over Southeast Asia: does 1.5°C or 2°C global warming make a difference? *Environ Res Lett* 14:044015. <https://doi.org/10.1088/1748-9326/aaf77e>
- Ge F, Zhu S, Luo H et al (2021) Future changes in precipitation extremes over Southeast Asia: insights from CMIP6 multi-model ensemble. *Environ Res Lett*. <https://doi.org/10.1088/1748-9326/abd7ad>
- Grimaldi S, Petroselli A, Baldini L, Gorgucci E (2018) Description and preliminary results of a 100 square meter rain gauge. *J Hydrol* 556:827–834. <https://doi.org/10.1016/j.jhydrol.2015.09.076>
- Gu L, Chen J, Yin J et al (2020) Responses of precipitation and runoff to climate warming and implications for future drought changes in China. *Earth's Futur*. <https://doi.org/10.1029/2020EF001718>
- Held IM, Soden BJ (2000) Water vapor feedback and global warming. *Annu Rev Energy Environ*. <https://doi.org/10.1146/annurev.energy.25.1.441>
- Hina S, Saleem F, Arshad A et al (2021) Droughts over Pakistan: possible cycles, precursors and associated mechanisms. *Geomat Nat Hazards Risk* 12:1638–1668. <https://doi.org/10.1080/19475705.2021.1938703>
- Hope TMH (2019) Linear regression. In: Mechelli A, Vieira S (eds) *Machine learning: methods and applications to brain disorders*. Academic Press, Cambridge
- Horton R, De Mel M, Peters D et al (2017) Assessing climate risks in Myanmar: summary for policymakers and planners
- Huang D, Yan P, Xiao X et al (2019) The tri-pole relation among daily mean temperature, atmospheric moisture and precipitation intensity over China. *Glob Planet Change* 179:1–9. <https://doi.org/10.1016/j.gloplacha.2019.04.016>
- Huo Y, Peltier WR (2020) Dynamically downscaled climate change projections for the South Asian monsoon: mean and extreme precipitation changes and physics parameterization impacts. *J Clim* 33:2311–2331. <https://doi.org/10.1175/JCLI-D-19-0268.1>
- Intergovernmental Panel on Climate Change (2014) *Climate change 2014 mitigation of climate change*. Cambridge University Press, Cambridge
- Iyakaremye V, Zeng G, Siebert A, Yang X (2021a) Contribution of external forcings to the observed trend in surface temperature over Africa during 1901–2014 and its future projection from CMIP6 simulations. *Atmos Res* 254:105512. <https://doi.org/10.1016/j.atmosres.2021.105512>

- Iyakaremye V, Zeng G, Yang X et al (2021b) Increased high-temperature extremes and associated population exposure in Africa by the mid-21st century. *Sci Total Environ* 790:148162. <https://doi.org/10.1016/j.scitotenv.2021.148162>
- Iyakaremye V, Zeng G, Zhang G (2021c) Changes in extreme temperature events over Africa under 1.5 and 2.0°C global warming scenarios. *Int J Climatol* 41:1506–1524. <https://doi.org/10.1002/joc.6868>
- Jiang J, Zhou T, Chen X, Zhang L (2020) Future changes in precipitation over Central Asia based on CMIP6 projections. *Environ Res Lett* 15:054009. <https://doi.org/10.1088/1748-9326/ab7d03>
- Kreft S, Eckstein D, Melchior I (2017) Global climate risk index 2017. Who suffers most from extreme weather events? Weather-related loss events in 2015 and 1996 to 2015. *Think Tank Res* 76:1–28
- Lai P, Zhang M, Ge Z et al (2020) Responses of seasonal indicators to extreme droughts in Southwest China. *Remote Sens*. <https://doi.org/10.3390/rs12050818>
- Lawrence MG (2005) The relationship between relative humidity and the dewpoint temperature in moist air: a simple conversion and applications. *Bull Am Meteorol Soc* 86:225–234. <https://doi.org/10.1175/BAMS-86-2-225>
- Liu M, Ma X, Yin Y et al (2021) Non-stationary frequency analysis of extreme streamflow disturbance in a typical ecological function reserve of China under a changing climate. *Ecohydrology* 23:1–20. <https://doi.org/10.1002/eco.2323>
- Mie Sein ZM, Islam ARMT, Maw KW, Moya TB (2015) Characterization of southwest monsoon onset over Myanmar. *Meteorol Atmos Phys*. <https://doi.org/10.1007/s00703-015-0386-0>
- Mie Sein ZM, Ullah I, Saleem F et al (2021a) Interdecadal variability in Myanmar rainfall in the monsoon season (May–October) using Eigen methods. *Water* 13:729. <https://doi.org/10.3390/w13050729>
- Mie Sein ZM, Ullah I, Syed S et al (2021b) Interannual variability of air temperature over Myanmar: the influence of ENSO and IOD. *Climate* 9:35. <https://doi.org/10.3390/cli9020035>
- Nasrollahi M, Khosravi H, Moghaddamnia A et al (2018) Assessment of drought risk index using drought hazard and vulnerability indices. *Arab J Geosci*. <https://doi.org/10.1007/s12517-018-3971-y>
- NECC and MECF (2012) Myanmar's national adaptation programme of action (NAPA) to climate change, p 126
- Nwe T, Zomer RJ, Corlett RT (2020) Projected impacts of climate change on the protected areas of Myanmar. *Climate* 8:1–15. <https://doi.org/10.3390/CLI8090099>
- Omer A, Zhuguo M, Zheng Z, Saleem F (2020) Natural and anthropogenic influences on the recent droughts in Yellow River Basin. *China Sci Total Environ* 704:135428. <https://doi.org/10.1016/j.scitotenv.2019.135428>
- Sadeghi SH, Peters TR, Cobos DR et al (2013) Direct calculation of thermodynamic wet-bulb temperature as a function of pressure and elevation. *J Atmos Ocean Technol*. <https://doi.org/10.1175/JTECH-D-12-00191.1>
- Samararathna KG, Abeywickrama ALKR, Hewawasam ISN et al (2017) Portable weather station. In: 2nd Undergrad Res Symp Fac Sci Univ Ruhuna
- Schmidt GA (2010) Enhancing the relevance of palaeoclimate model/data comparisons for assessments of future climate change. *J Quat Sci* 25:79–87. <https://doi.org/10.1002/jqs.1314>
- Sein ZMM, Zhi X (2016) Interannual variability of summer monsoon rainfall over Myanmar. *Arab J Geosci* 9:469. <https://doi.org/10.1007/s12517-016-2502-y>
- Sein ZMM, Zhi X, Ogou FK et al (2021) Spatio-temporal analysis of drought variability in Myanmar based on the standardized precipitation evapotranspiration index (SPEI) and its impact on crop production. *Agronomy* 11:1691. <https://doi.org/10.3390/agronomy11091691>
- Seong M-G, Min S-K, Kim Y-H et al (2020) Anthropogenic greenhouse gas and aerosol contributions to extreme temperature changes during 1951–2015. *J Clim*. <https://doi.org/10.1175/JCLI-D-19-1023.1>
- Shahzaman M, Zhu W, Bilal M et al (2021a) Remote sensing indices for spatial monitoring of agricultural drought in south Asian countries. *Remote Sens* 13:2059. <https://doi.org/10.3390/rs1312059>
- Shahzaman M, Zhu W, Ullah I et al (2021b) Comparison of multi-year reanalysis, models, and satellite remote sensing products for agricultural drought monitoring over south Asian countries. *Remote Sens* 13:3294. <https://doi.org/10.3390/rs13163294>
- Shi X, Chen J, Gu L et al (2021) Impacts and socioeconomic exposures of global extreme precipitation events in 1.5 and 2.0°C warmer climates. *Sci Total Environ* 766:142665. <https://doi.org/10.1016/j.scitotenv.2020.142665>
- Shim S, Kim J, Sung HM et al (2021) Future changes in extreme temperature and precipitation over East Asia under SSP scenarios. *J Clim Chang Res* 12:143–162. <https://doi.org/10.15531/kscrcr.2021.12.2.143>
- Shrestha AK, Thapa A, Gautam H (2019) Solar radiation, air temperature, relative humidity, and dew point study: Damak, Jhapa, Nepal. *Int J Photoenergy* 2019:8369231. <https://doi.org/10.1155/2019/8369231>
- Simões-Moreira JR (1999) A thermodynamic formulation of the psychrometer constant. *Meas Sci Technol*. <https://doi.org/10.1088/0957-0233/10/4/008>
- Suman M, Maity R (2020) Southward shift of precipitation extremes over south Asia: evidences from CORDEX data. *Sci Rep* 10:6452. <https://doi.org/10.1038/s41598-020-63571-x>
- Trenberth KE, Stepaniak DP (2003) Covariability of components of poleward atmospheric energy transports on seasonal and interannual timescales. *J Clim*. [https://doi.org/10.1175/1520-0442\(2003\)016%3c3691:COCOPA%3e2.0.CO;2](https://doi.org/10.1175/1520-0442(2003)016%3c3691:COCOPA%3e2.0.CO;2)
- Ukhurebor KE, Abiodun IC, Bakare F (2017) Relationship between relative humidity and the dew point temperature in Benin City, Nigeria. *J Appl Sci Environ Manage* 21(5):953–956. <https://doi.org/10.4314/jasem.v21i5.22>
- Ullah I, Ma X, Yin J et al (2021a) Evaluating the meteorological drought characteristics over Pakistan using In-situ observations and reanalysis products. *Int J Climatol* 41(9):4437–4459. <https://doi.org/10.1002/joc.7063>
- Ullah I, Ma X, Yin J et al (2021b) Observed changes in seasonal drought characteristics and their possible potential drivers over Pakistan. *Int J Climatol*. <https://doi.org/10.1002/joc.7321>
- Wang B, Ding Q, Joseph PV (2009) Objective definition of the Indian summer monsoon onset. *J Clim* 22:3303–3316. <https://doi.org/10.1175/2008JCLI2675.1>
- Wentz FJ, Schabel M (2000) Precise climate monitoring using complementary satellite data sets. *Nature*. <https://doi.org/10.1038/35000184>
- Wilks DS (2007) *Statistical methods in the atmospheric sciences*, 2nd edn. Academic Press, Cambridge
- Zhang Q, Wang S, Yue P, Wang S (2019) Variation characteristics of non-rainfall water and its contribution to crop water requirements in China's summer monsoon transition zone. *J Hydrol* 578:124039. <https://doi.org/10.1016/j.jhydrol.2019.124039>
- Zheng Y, He Y, Chen X (2017) Spatiotemporal pattern of precipitation concentration and its possible causes in the Pearl River basin, China. *J Clean Prod* 161:1020–1031. <https://doi.org/10.1016/j.jclepro.2017.06.156>
- Zheng Y, Zhang Q, Luo M et al (2020) Wintertime precipitation in eastern China and relation to the Madden-Julian oscillation:

spatiotemporal properties, impacts and causes. *J Hydrol* 582:124477. <https://doi.org/10.1016/j.jhydrol.2019.124477>

Zhu S, Ge F, Sein DV (2019) Projected changes in surface air temperature over the Indochina Peninsula from the regionally coupled model ROM Projected changes in surface air temperature over the Indochina Peninsula from the regionally coupled model ROM

Zhu S, Ge F, Fan Y et al (2020) Conspicuous temperature extremes over Southeast Asia: seasonal variations under 1.5 °C and 2 °C

global warming. *Clim Change* 160:343–360. <https://doi.org/10.1007/s10584-019-02640-1>

Publisher's Note Springer Nature remains neutral with regard to jurisdictional claims in published maps and institutional affiliations.